Two-magnon states of the alternating ferromagnetic Heisenberg chain

1989 J. Phys.: Condens. Matter 1 9899

(http://iopscience.iop.org/0953-8984/1/49/010)

J. Phys.: Condens. Matter 1 (1989) 9899–9910. Printed in the UK

Two-magnon states of the alternating ferromagnetic Heisenberg chain

S C Bell†, P D Loly and B W Southern
Department of Physics, University of Manitoba, Winnipeg, Manitoba, Canada R3T 2N2

Received 14 June 1989

Abstract. In this paper we examine the nature of two-magnon excitations in the alternating bond ferromagnetic $S = \frac{1}{2}$ spin chain. Both a direct analytic approach as well as a method based on a scaling transformation are used to study the bound state branches and their relationship to the two-magnon continuum. Several features are expected to be observable in two-magnon Raman scattering experiments.

1. Introduction

In this paper we study the nature of the excitations in the $S = \frac{1}{2}$ alternating bond ferromagnetic Heisenberg spin chain. It is well known from the work of Bethe [1] that the uniform ferromagnetic chain has a two-magnon bound state which lies below a single continuum of two-magnon scattering states for all values of the total wavevector K and that the energy of this state is equal to one half of the one-magnon state. In a chain with alternating bond strengths the usual sinsuoidal spin-wave, or one-magnon, spectrum is split up into two branches, which we shall call the 'acoustic' and 'optic' modes by analogy with the diatomic chain model in lattice dynamics. Three separate two-magnon continua therefore follow from the non-interacting combinations of the optic and acoustic branches and are separated by gaps when plotted as a function of energy and total wavevector. Our interest in this paper is to determine the structure of the two-magnon spectra resulting from the interaction between these different branches of magnons. The dispersion relations of the bound states have been studied previously by Krupennikov [2] using a direct analytic approach. He then solves the resulting equations using first-order perturbation theory in the limit of both strong and weak bond alternation. We find that the two-magnon spectrum is much more complicated than one would expect based on his results and also in comparison with other models which have already been solved, such as the next-nearest-neighbour (NNN) ferromagnetic chain [3].

We carry out our calculations using two different methods: firstly we use a direct analytic approach which can be considered as a generalisation of the Bethe *ansatz* [1] for the uniform chain and secondly we use a scaling approach recently introduced by Southern *et al* [4]. Our analytic approach is closely related to the work of Krupennikov [2] but there are some important differences in the final results. In particular, we find that a bound state exists in one of the gaps at $K = 0$ and is possibly a good candidate

† Present address: ICI Paints, Research Department, Wexham Road, Slough, Berkshire SL2 5DS, UK.

0953-8984/89/499899+12$02.50

for detection by a light-scattering experiment. The scaling method is well suited to the calculation of response functions, including the bound states, and can be used to investigate resonant states inside the continuum. It is also easily extended to higher values of the spin.

In section 2 we write down the basic set of equations for the two-magnon excitations and show how the calculation of the bound-state energies reduces to the solution of a constraint equation. We discuss the nature of the solution in the various regions of energy and total wavevector. In section 3 we solve for the bound states numerically and plot the branches. The scaling approach is described in section 4 where results for resonant states are also described. In concluding with section 5 we consider the possibility of extending the analytic calculation to the antiferromagnetic version of the model which has important applications in spin–Peierls theory [5].

2. The model and its formal solution

The Hamiltonian for the alternating ferromagnetic Heisenberg spin chain is given by

$$H = -\sum_{n=1}^{N/2} (J_1 \boldsymbol{S}_{2n} \cdot \boldsymbol{S}_{2n+1} + J_2 \boldsymbol{S}_{2n+1} . \boldsymbol{S}_{2n+2}) \tag{1}$$

where $\boldsymbol{S}_m$ are the usual $S = \frac{1}{2}$ Pauli operators associated with site m and J_1, J_2 are the bond strengths, both of which will be taken to be positive. We shall assume that $J_2 \leq J_1$ without loss of generality. The ground state of this model is the completely aligned state and the magnetisation will be chosen to be along the z axis.

The spin-wave, or one-magnon, states can be written as

$$|\psi\rangle = \sum_n [a_{2n}|2n\rangle + a_{2n+1}|2n+1\rangle] \tag{2}$$

where the ket $|n\rangle$ represents the state with the nth spin flipped relative to the ground state. Substituting this expression into the Schrödinger equation $H|\psi\rangle = E|\psi\rangle$ we obtain the following equations for the amplitudes a_{2n} and a_{2n+1}:

$$\begin{aligned} 2Ea_{2n} &= (J_1 + J_2)a_{2n} - (J_1 a_{2n-1} + J_2 a_{2n+1}) \\ 2Ea_{2n+1} &= (J_1 + J_2)a_{2n+1} - (J_1 a_{2n+2} + J_2 a_{2n}) \end{aligned} \tag{3}$$

where the energy E of the one-magnon state is measured relative to the ground state energy $E_0 = -(J_1 + J_2)N/8$ and we have set $\hbar = 1$. This pair of equations is formally identical to that obtained for phonons on a diatomic chain [6]. The solution can be written as

$$\begin{aligned} a_{2n} &= \alpha \exp(2\mathrm{i}nk) \\ a_{2n+1} &= \beta \exp(\mathrm{i}(2n+1)k) \end{aligned} \tag{4}$$

with $-\pi/2 < k < \pi/2$. The dispersion relation [2] is

$$E_k^\mu = \tfrac{1}{2}J_1 + \tfrac{1}{2}J_2 + \tfrac{1}{2}\mu\sqrt{J_1^2 + J_2^2 + 2J_1J_2\cos 2k} \tag{5}$$

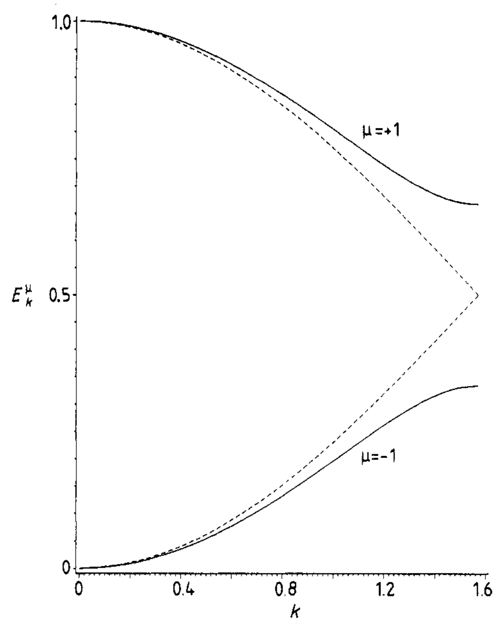

Figure 1. The two branches ($\mu = \pm 1$) of the one-magnon dispersion curve for the alternating bond chain with $J_2/J_1 = 0.5$ (full curve) and $J_2 = J_1$ (broken curve). The energy is in units of $(J_1 + J_2)$.

where $\mu = \pm 1$ labels the two branches. We shall designate the upper branch ($\mu = +1$) of this relation 'optic' and the lower branch ($\mu = -1$) 'acoustic' by analogy with the phonon problem. These branches are shown in figure 1. There is a gap between the branches at $k = \pi/2$ which is equal to $J_1 - J_2$. We anticipate that the two-magnon excitation spectrum will exhibit similar behaviour.

The two-magnon state can be written as

$$|\psi\rangle = \sum_{n \leq m} [a_{2n,2m}|2n, 2m\rangle + a_{2n,2m+1}|2n, 2m+1\rangle + a_{2n-1,2m}|2n-1, 2m\rangle + a_{2n+1,2m+1}|2n+1, 2m+1\rangle] \tag{6}$$

where the amplitudes for the four possible configurations of the excitations (even–even, even–odd, odd–even, odd–odd) have been written separately. The even–even and odd–odd amplitudes with $m = n$ are unphysical for $S = \frac{1}{2}$ but are retained because they can be used to simplify the solution which follows. Substituting in the Schrödinger equation we obtain the following equations for the amplitudes if $m > n$:

$$\begin{aligned}
2\Omega a_{2n,2m} &= -J_1(a_{2n,2m+1} + a_{2n+1,2m}) - J_2(a_{2n,2m-1} + a_{2n-1,2m}) \\
2\Omega a_{2n+1,2m+1} &= -J_1(a_{2n,2m+1} + a_{2n+1,2m}) - J_2(a_{2n+2,2m+1} + a_{2n+1,2m+2}) \\
2\Omega a_{2n-1,2m} &= -J_1(a_{2n-2,2m} + a_{2n-1,2m+1}) - J_2(a_{2n-1,2m-1} + a_{2n,2m}) \\
2\Omega a_{2n,2m+1} &= -J_1(a_{2n,2m} + a_{2n+1,2m+1}) - J_2(a_{2n-1,2m+1} + a_{2n,2m+2})
\end{aligned} \tag{7}$$

whereas if $m = n$, we have

$$\begin{aligned}
2(\Omega + J_2)a_{2n-1,2n} &= -J_1(a_{2n-2,2n} + a_{2n-1,2n+1}) \\
2(\Omega + J_1)a_{2n,2n+1} &= -J_2(a_{2n-1,2n+1} + a_{2n,2n+2}).
\end{aligned} \tag{8}$$

We have used the variable $\Omega = E - J_1 - J_2$ to simplify the expressions. The first set of equations is valid for separations greater than one and so describes non-interacting magnons. The second set of equations takes into account the possibility of the flipped spins being adjacent; this results in different equations which we shall call the constraint equations. Following Bethe's fundamental work on the antiferromagnetic chain we can express the constraints in (8) as follows [1, 2]:

$$\begin{aligned} 2a_{2n,2n+1} &= a_{2n,2n} + a_{2n+1,2n+1} \\ 2a_{2n-1,2n} &= a_{2n-1,2n-1} + a_{2n,2n} \end{aligned} \tag{9}$$

using the unphysical amplitudes representing spin flips on the same site. The equations now have the form of the non-interacting magnon case for all $m \geq n$ and it is possible to solve them by a generalisation of the one-magnon wavefunction for the diatomic chain

$$\begin{aligned} a_{2n,2m} &= \alpha \exp(2ik_1 n + 2ik_2 m) \\ a_{2n-1,2m} &= \beta \exp(ik_1(2n-1) + 2ik_2 m) \\ a_{2n,2m+1} &= \gamma \exp(2ik_1 n + ik_2(2m+1)) \\ a_{2n+1,2m+1} &= \delta \exp(ik_1(2n+1) + ik_2(2m+1)) \end{aligned} \tag{10}$$

where k_1 and k_2 are the wavevectors of the individual magnons. Substituting this into the non-interacting equations produces a matrix eigenvalue equation

$$\begin{pmatrix} \Omega & A_+ & B_+ & 0 \\ A_- & \Omega & 0 & B_+ \\ B_- & 0 & \Omega & A_+ \\ 0 & B_- & A_- & \Omega \end{pmatrix} \begin{pmatrix} \alpha \\ \beta \\ \gamma \\ \delta \end{pmatrix} = 0 \tag{11}$$

with

$$\begin{aligned} 2A_\pm &= J_1 \exp(\pm ik_1) + J_2 \exp(\mp ik_1) \\ 2B_\pm &= J_1 \exp(\pm ik_2) + J_2 \exp(\mp ik_2) \end{aligned} \tag{12}$$

The secular equation is

$$\Omega^4 - 2\Omega^2(|A|^2 + |B|^2) + (|A|^2 - |B|^2)^2 = 0 \tag{13}$$

where $|A|^2 = A_+A_-$ and $|B|^2 = B_+B_-$. Note that $|A|^2$ and $|B|^2$ will only be real if k_1 and k_2 are real, otherwise they are complex. The secular equation can be solved for Ω and hence the two-magnon excitation energy E yielding

$$E_{K,q}^{\mu_1,\mu_2} = E_{k_1}^{\mu_1} + E_{k_2}^{\mu_2} \tag{14}$$

where K and q are the total and relative wavevectors defined as $K = k_1 + k_2$ and $2q = k_1 - k_2$ respectively. The indices μ_1 and μ_2 take the values ± 1 independently and label the various branches of the two-magnon spectrum. This expression is clearly just the sum of the energy of two non-interacting magnons. The corresponding eigenvectors for each branch are

$$\begin{aligned} \alpha &= \mu_1\mu_2(A_+B_+/|A||B|)\delta \\ \beta &= -\mu_2(B_+/|B|)\delta \\ \gamma &= -\mu_1(A_+/|A|)\delta. \end{aligned} \tag{15}$$

We can plot the regions in the E versus K plane that correspond to real values of k_1 and k_2 (or q). Figure 2(a) shows the boundaries of the various continua derived from (14). These boundaries can be calculated explicitly by finding the turning points of the expression for the energy as a function of q. The upper boundary of the optic–optic (O–O) continuum ($\mu_1 = \mu_2 = +1$) and the lower boundary of the acoustic–acoustic (A–A) continuum ($\mu_1 = \mu_2 = -1$) are given by the pair of curves

$$E_{1,\pm} = J_1 + J_2 \pm \sqrt{J_1^2 + J_2^2 + 2J_1J_2\cos K} \tag{16}$$

and correspond to $q = 0$. The lower boundary of the O–O continuum and the upper boundary of the A–A continuum correspond to $q = \pi/2$ and are given by

$$E_{2,\pm} = J_1 + J_2 \pm \sqrt{J_1^2 + J_2^2 - 2J_1J_2\cos K} \tag{17}$$

but *only* for $K < K_c = \cos^{-1}(J_2/J_1)$. Thereafter these two curves correspond to internal van Hove singularities within the respective continua. For $K > K_c$ the boundaries are given by

$$E_{3,\pm} = J_1 + J_2 \pm J_1 \sin K. \tag{18}$$

In this case q is now given by the expression $\cos 2q = -(J_1/J_2)\cos K$, so q changes continuously from $\pi/2$ at K_c to $\pi/4$ at the zone boundary. The mixed-mode continuum ($\mu_1 = -\mu_2$) has boundaries

$$E_{4,\pm} = J_1 + J_2 \pm J_2 \sin K \tag{19}$$

and q is given by $\cos 2q = -(J_2/J_1)\cos K$ for all K.

An alternative approach [2] to finding the boundaries of the continua is to solve the secular equation (13) for $\cos 2q$:

$$\cos 2q = \frac{-\Omega^2 \cos K \pm \sqrt{(\Omega^2 - J_1^2\sin^2 K)(\Omega^2 - J_2^2 \sin^2 K)}}{J_1J_2\sin^2 K} \tag{20}$$

In general there are four complex values of q (occurring in complex conjugate pairs) for each value of Ω (or E) and K. By considering the conditions for which q is real the boundaries can be recovered from this expression. Figure 2(b) shows the various regions of the E versus K plane as labelled by Krupennikov [2]. In regions I, III and V the physical solutions correspond to complex values of q whereas in regions II, IV and VI some of the values of q are real.

Having studied the non-interacting problem in some detail it is now possible to consider the constraint equations. To solve the complete set of equations (7) and (9)

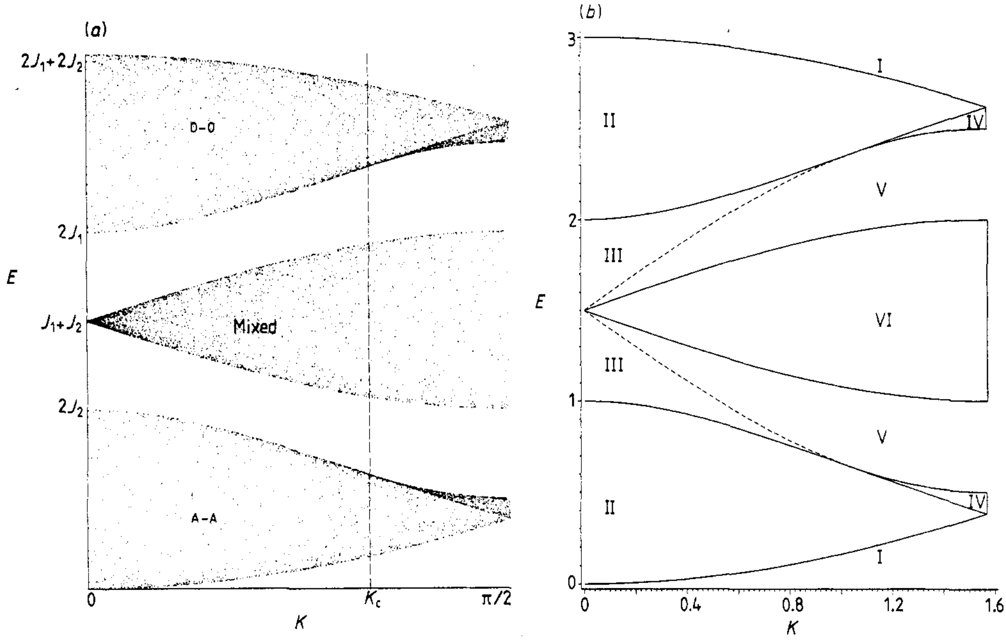

Figure 2. (*a*) The two-magnon continuum branches and their boundaries. The vertical broken line indicates K_c. (*b*) Regions of the E versus K plane. The broken curve separating regions III and V is given by equation (18). The energy is in units of J_1 and $J_2 = 0.5J_1$.

we have to take non-interacting solutions and use a matching procedure to satisfy the constraint equations. However, in the limit of an infinite chain, we must reject solutions that correspond to exponentially increasing amplitudes. In the regions outside the continua, there are only two values of q, q and $\overline{q}$, for every choice of E and K.

To find the bound state energies we write the amplitudes as linear combinations of these solutions

$$a_{2n,2m} = \exp(\mathrm{i}K(n+m))[C\alpha\exp(-\mathrm{i}q(2m-2n)) + D\overline{\alpha}\exp(-\mathrm{i}\overline{q}(2m-2n))]$$
$$a_{2n-1,2m} = \exp(\mathrm{i}K(n+m-\tfrac{1}{2}))[C\beta\exp(-\mathrm{i}q(2m-2n+1)) + D\overline{\beta}\exp(-\mathrm{i}\overline{q}(2m-2n+1))]$$
$$a_{2n,2m+1} = \exp(\mathrm{i}K(n+m+\tfrac{1}{2}))[C\gamma\exp(-\mathrm{i}q(2m-2n+1)) + D\overline{\gamma}\exp(-\mathrm{i}\overline{q}(2m-2n+1))]$$
$$a_{2n+1,2m+1} = \exp(\mathrm{i}K(n+m+1))[C\delta\exp(-\mathrm{i}q(2m-2n)) + D\overline{\delta}\exp(-\mathrm{i}\overline{q}(2m-2n))] \qquad (21)$$

where C and D are arbitrary constants and q and $\overline{q}$ are the two values of the relative wavevector appropriate to the chosen values of E and K. Since $m \geq n$ we must choose the imaginary parts of the q and $\overline{q}$ to be negative. The coefficients $\alpha, \beta, \gamma, \delta$ and the corresponding barred quantities are given by (15) once q and $\overline{q}$ are determined. For finite chains both the exponentially rising and decaying terms would have to be included. The expression for the amplitudes with these additional terms would be in the form of a generalised Bethe *ansatz* [1]. Substituting (21) into the constraint equations and eliminating C and D we obtain

$$\frac{\alpha\exp(-\frac{1}{2}\mathrm{i}K) + \delta\exp(\frac{1}{2}\mathrm{i}K) - 2\gamma\exp(-\mathrm{i}q)}{\overline{\alpha}\exp(-\frac{1}{2}\mathrm{i}K) + \overline{\delta}\exp(\frac{1}{2}\mathrm{i}K) - 2\overline{\gamma}\exp(-\mathrm{i}\overline{q})} = \frac{\alpha\exp(\frac{1}{2}\mathrm{i}K) + \delta\exp(-\frac{1}{2}\mathrm{i}K) - 2\beta\exp(-\mathrm{i}q)}{\overline{\alpha}\exp(\frac{1}{2}\mathrm{i}K) + \overline{\delta}\exp(-\frac{1}{2}\mathrm{i}K) - 2\overline{\beta}\exp(-\mathrm{i}\overline{q})}. \qquad (22)$$

To solve (22) for the two-magnon bound states we have numerically scanned with respect to E through regions I, III and V in figure 2(*b*) for fixed values of K. The solution of this equation will be considered in the next section.

3. Dispersion relation of the bound states

In region I, below the A–A continuum, we obtain bound states which are most easily understood by first considering the spectrum of the uniform bond chain in the reduced Brillouin zone $-\pi/2 < K < \pi/2$. The usual bound state below the continuum is folded back at $K = \pi/2$ and consists of a lower and upper part which meet at the Brillouin zone boundary with no gap (see figure 3(*a*)). The upper part of this state is a true bound state even though it lies in the same region of energy as the continuum states.

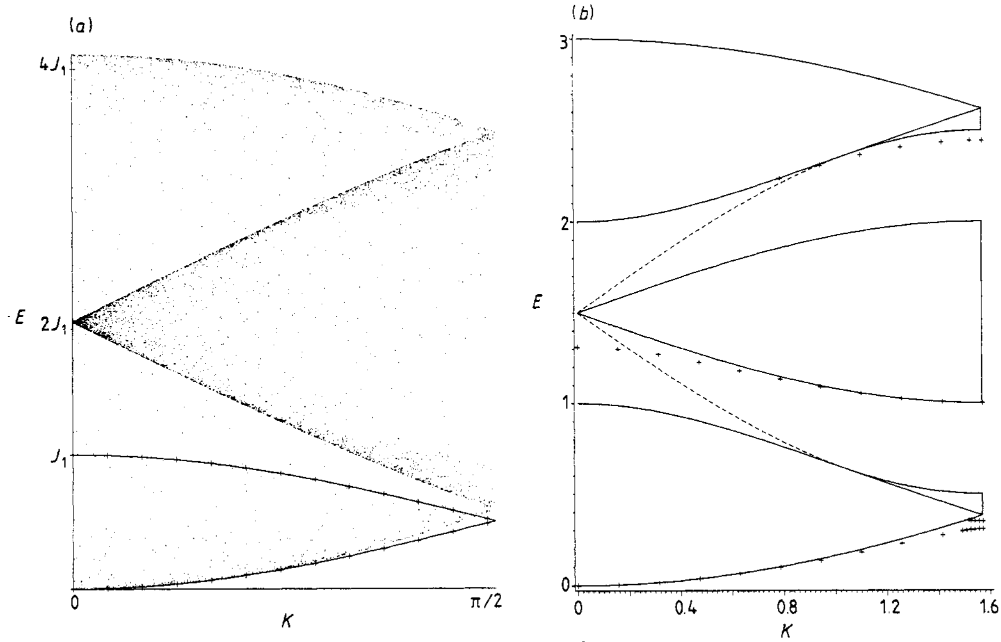

Figure 3. (*a*) The two-magnon continuum (shaded region) and the bound state branch (crosses) of the uniform chain in the reduced zone. (*b*) The bound state branches (crosses) of the alternating bond chain for for $J_2/J_1 = 0.5$. The broken curve separates regions III and V as in figure 2(*b*).

Figure 3(*b*) shows our results for the various bound state branches for $J_2/J_1 = 0.5$. In the alternating bond case, the lower state remains a true bound state but the upper state becomes a resonant state inside the continuum (region II of figure 2(*b*)). Near $K = \pi/2$ the upper state emerges below the continuum as a true bound state and is separated from the lower state by a gap at the Brillouin zone boundary. In the uniform limit, the gap between these two bound states vanishes linearly with $J_1 - J_2$ and the resonant state becomes a bound state for all values of K. These results agree with those of Krupennikov [2] except for the presence of a gap at the zone boundary. He used first order perturbation theory about the uniform limit but his results are not correct at

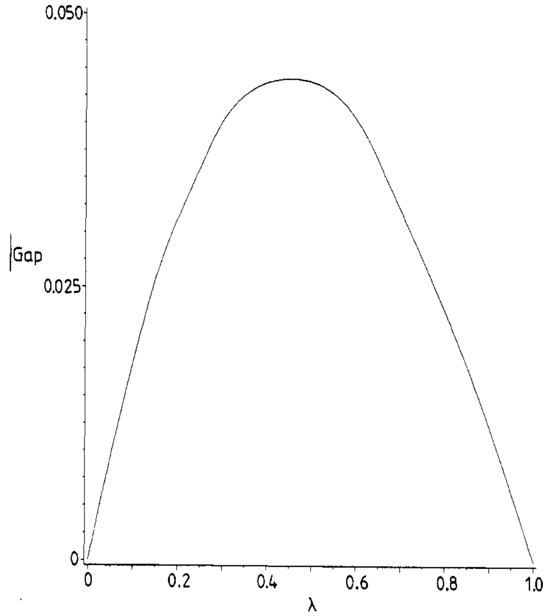

Figure 4. The gap between the A–A bound states at $K = \pi/2$ as a function of $\lambda = (J_1 - J_2)/(J_1 + J_2)$.

the first reduced Brillouin zone boundary where degenerate second order perturbation theory must be used. Figure 4 shows how the gap varies with $\lambda = (J_1 - J_2)/(J_1 + J_2)$.

In regions III and V of figure 3(*b*) we obtain another bound state branch below the mixed continuum. This state exists for all K and meets the continuum at $K = \pi/2$. However, for all $K > K_c$ the binding energy is extremely small. This bound state is a good candidate for observation using optical techniques. The binding energy of this state at $K = 0$ as a function of λ is similar to the curve in figure 4.

A final bound state branch exists in region V below the O–O continuum. This branch emerges from the O–O continuum into region III at a value of K slightly less than K_c. At smaller values of K the state is a resonant state at the lower edge of the continuum. Again, the binding energy of this state at $K = \pi/2$ is similar to the result in figure 4. Both of the branches which lie in the continuum gaps change their character as they cross from region III to region V with increasing K. This is due to the fact that the two values of q are degenerate at the boundary of these regions. In region III the imaginary parts of q and $\bar{q}$ are different and the bound bound is a superposition of two exponentially decaying functions. In region V the imaginary parts of the two values of q are the same but the real parts are different.

We have therefore found bound state branches that we can associate with each continuum. The evolution of the branches as a function of the ratio of J_2 to J_1 is more complicated than the perturbation results of Krupennikov[2] would suggest.

4. Scaling treatment of two-magnon excitations

In the previous sections we have described an analytic approach to the solution of the Schrödinger equation. The treatment essentially consisted of expanding the interacting two-magnon states in terms of the non-interacting one-magnon states. In this section we will describe a scaling approach to the problem which does not rely upon solving the one-magnon problem beforehand. This scaling approach has recently been used by Southern *et al* [4] to study the two-magnon excitations in general S quantum spin chains with uniform bonds and is easily extended to the alternating chain.

We first express the four different types of amplitudes in (6) in terms of their centre of mass and relative coordinates as follows:

$$\begin{aligned}
a_{2n,2m} &= u^{(1)}_{2(m-n)} \exp(\mathrm{i}K(2n+2m)/2) \\
a_{2n-1,2m} &= u^{(2)}_{2(m-n)+1} \exp(\mathrm{i}K(2n+2m-1)/2) \\
a_{2n,2m+1} &= u^{(3)}_{2(m-n)+1} \exp(\mathrm{i}K(2n+2m+1)/2) \\
a_{2n+1,2m+1} &= u^{(4)}_{2(m-n)} \exp(\mathrm{i}K(2n+2m+2)/2)
\end{aligned} \tag{23}$$

where K is the total wavevector of the two-magnon state. The four amplitudes for the relative coordinates are now defined to be the components of a vector as follows:

$$U_{2r} = \begin{pmatrix} u^{(1)}_{2r} \\ u^{(2)}_{2r+1} \\ u^{(3)}_{2r+1} \\ u^{(4)}_{2r} \end{pmatrix} \qquad r = 0, 1, 2 \ldots . \tag{24}$$

Equations (7) and (8) can now be expressed concisely as

$$\begin{aligned}
MU_{2r} &= V_p U_{2r+2} + V_m U_{2r-2} \qquad r > 0 \\
M_0 U_0 &= V_p U_2 \qquad r = 0.
\end{aligned} \tag{25}$$

The matrices M, M_0, V_p, V_m have the following form:

$$\begin{aligned}
M &= \begin{pmatrix} \Omega & c_2^* & c_1 & 0 \\ c_2 & \Omega & 0 & c_2^* \\ c_1^* & 0 & \Omega & c_1 \\ 0 & c_2 & c_1{*} & \Omega \end{pmatrix} \qquad
M_0 = \begin{pmatrix} \Omega & 0 & 0 & 0 \\ 0 & \Omega + J_2 & 0 & 0 \\ 0 & 0 & \Omega + J_1 & 0 \\ 0 & 0 & 0 & \Omega \end{pmatrix} \\
V_p &= \begin{pmatrix} 0 & 0 & 0 & 0 \\ -c_1^* & 0 & 0 & -c_1 \\ -c_2 & 0 & 0 & -c_2^* \\ 0 & 0 & 0 & 0 \end{pmatrix} \qquad
V_m = \begin{pmatrix} 0 & -c_1 & -c_2^* & 0 \\ 0 & 0 & 0 & 0 \\ 0 & 0 & 0 & 0 \\ 0 & -c_1^* & -c_2 & 0 \end{pmatrix}
\end{aligned} \tag{26}$$

where $c_1 = \frac{1}{2}J_1 \exp(\frac{1}{2}\mathrm{i}K)$ and $c_2 = \frac{1}{2}J_2 \exp(\frac{1}{2}\mathrm{i}K)$.

The scaling approach involves performing a transformation on these equations which leaves their form invariant but reduces the number of degrees of freedom. If we choose the vector U_0 as our origin and eliminate every second column vector, then the equations can be rewritten in the same form with the matrices M, M_0, V_p, V_m redefined as

$$\begin{aligned}
M' &= M - V_m M^{-1} V_p - V_p M^{-1} V_m \\
M_0' &= M_0 - V_p M^{-1} V_m \\
V_p' &= V_p M^{-1} V_p \\
V_m' &= V_m M^{-1} V_m .
\end{aligned} \tag{27}$$

The above transformation corresponds to a decimation procedure and has a scaling factor $b = 2$. The spectral properties of the system are determined by iterating the transformation but a small positive imaginary part must be used in the excitation energy for convergence. Under iteration, the matrices V_p and V_m approach zero (due to the complex energy) and hence the non-trivial solutions for the vector U_0 are determined from $\mathrm{Det}(M_0^{(\infty)}) = 0$.

If we add an inhomogeneous term to the equations (25), then we can use the above procedure to calculate the following two-magnon Green functions

$$G^{i,j}_{2r,2s}(E,K) = \langle u^{(i)}_{2r}| \frac{1}{E-H} |u^{(j)}_{2s}\rangle \tag{28}$$

where $i,j = 1,4$. For example, if we add a column vector with a non-zero entry only in the jth row to the right-hand side of the equation for U_0 in (25), the iteration procedure yields $G^{i,j}_{0,0}$. Figure 5 shows the imaginary part of various response functions at fixed $K = \pi/10$ for $J_2/J_1 = 0.5$ plotted as a function of energy. We have taken $J_1 = 1.0$ and a small imaginary part (10^{-5}) has been used in the energy. Within the regions of energy corresponding to the continuum states, 20 iterations are typically required for convergence. The imaginary parts of $G^{2,2}_{0,0}$ and $G^{3,3}_{0,0}$ describe the local densities of states for excitations on nearest-neighbour sites separated by the weak (J_2) and strong (J_1) bonds respectively. The imaginary part of $G^{1,1}_{2,2}$ describes the case when the spin deviations are separated by two sites. All three response functions are sensitive to the A–A bound state just below the lower edge of the A–A continuum and a rather sharp resonant peak appears in each near $E = 0.6$. The mixed-mode bound state contributes to each just below the mixed continuum with the largest weight appearing in the response function which corresponds to two deviations separated by the strong bond J_1. All three response functions in figure 5 also show contributions from both the mixed-mode and optic–optic continua. There is a resonant state at the lower edge of the O–O continuum which emerges as a true bound state at larger K.

As J_2 approaches J_1, the gaps between the continua vanish along with their bound states. However, the A–A resonance sharpens up and becomes a true bound state (see figure 3(a)).

5. Summary

We have found the complete solution to the two-magnon spectrum of the alternating $S = \frac{1}{2}$ ferromagnetic Heisenberg chain. From both the analytic solution and the scaling calculations we see that this model has three bound state branches, two of which are additional to those appearing in the uniform chain. The methods described here are easily extended to $S > \frac{1}{2}$ and Hamiltonians which include both exchange and single-ion anisotropies. Based on previous studies [7, 8] of the uniform chain, the presence of these terms could yield additional bound states in the alternating bond case as well. Alternating interactions can also occur in layered materials which can exhibit quasi-one-dimensional character [9] and other materials may well be grown synthetically in a layered manner by molecular beam epitaxy. The A–A resonance and the mixed-mode bound state for $K \simeq 0$ may be observable in light absorption or two-magnon Raman scattering experiments similar to those done in anisotropic but non-alternating quasi-one-dimensional magnets [10].

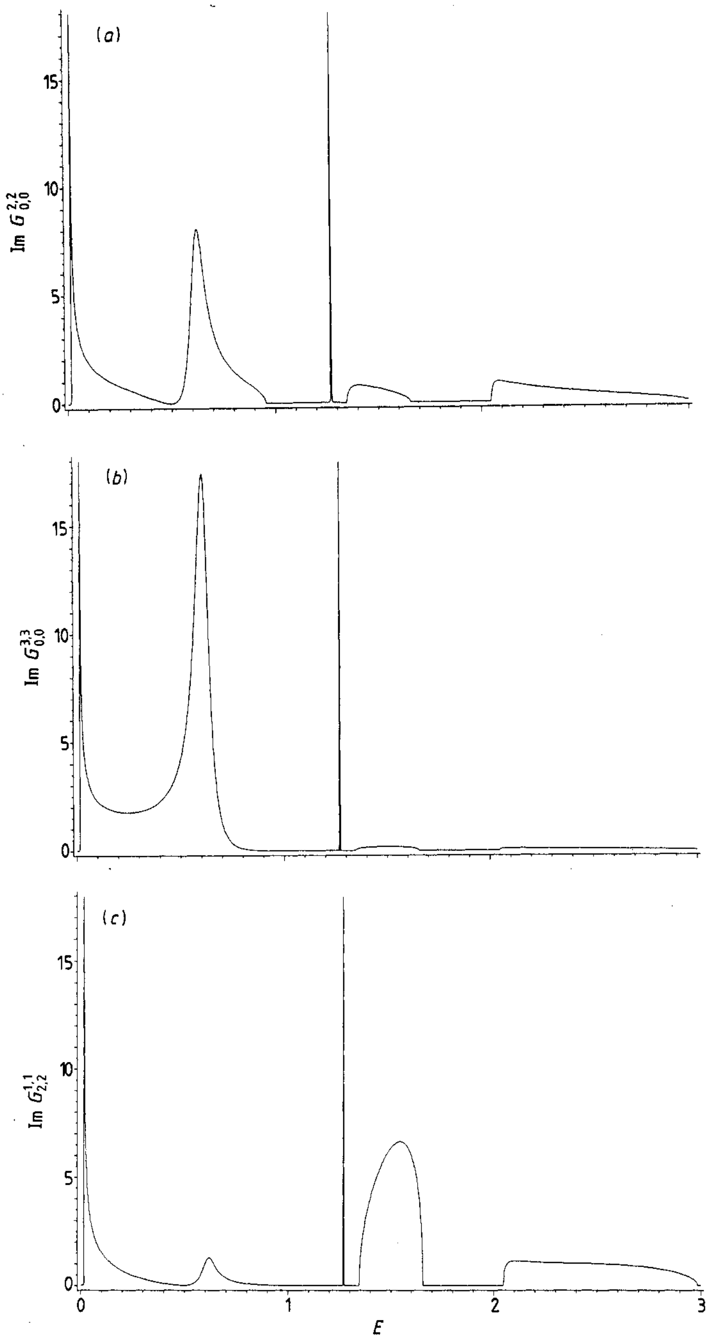

Figure 5. The local densities of states at $K = \pi/10$ for two spin deviations separated by (a) a strong bond J_1, (b) a weak bond J_2 and (c) two bonds.

One of the reasons for considering the alternating bond model was as a first step towards studying the excitations of the alternating antiferromagnetic chain. The solution of the alternating bond antiferromagnetic model would require the solution of the m-magnon problem for arbitrary m. The energy of the non-interacting magnons will be a sum of m-terms as in (14) with m wavevectors to be determined. However our results suggest that the alternating antiferromagnetic chain is non-integrable. Haldane [11] has conjectured that for Heisenberg spin chains to be integrable their m-magnon bound state dispersion curves must be continuous over $\min(m, 2S)$ Brillouin zones. This clearly does not hold for the alternating chain since the A–A bound state has a gap at the first reduced Brillouin zone boundary. We therefore believe that no further progress can be made towards an exact solution of the alternating antiferromagnetic chain using an approach based on the Bethe *ansatz*.

Finite size calculations [5] have shown that the $S = \frac{1}{2}$ alternating bond antiferromagnetic model has a gap appearing in the spin-wave spectrum at $K = 0$ in contrast to the uniform bond model which is gapless. This difference can be understood as a result of non-linear zero-point fluctuations, and is closely related to the so called 'Haldane' gap [12] in the $S = 1$ uniform antiferromagnetic chain. In fact the alternating chain can be thought of as a specific representation of that model as it has a unit cell containing integer spin albeit zero *or* one. Recently Krivoruchko [13] has studied the role of quantum fluctuations in a chain composed of two types of alternating spins. The ferromagnetic version of this latter model in which the spin magnitude rather than the exchange bond magnitude alternates should also exhibit two-magnon spectra similar to the results reported here.

Acknowledgments

This work was supported by the Natural Sciences and Engineering Research Council of Canada and the Research Board of the University of Manitoba.

References

[1] Bethe H A 1931 *Z. Phys.* **71** 205–26
[2] Krupennikov N A 1979 *Phys. Met. Metall.* **44** 10–9
[3] Bahurmuz A A and Loly P D 1986 *J. Phys. C: Solid State Phys.* **19** 2241–52
[4] Southern B W, Liu T S and Lavis D A 1989 *Phys. Rev.* B **39** 12160–4
[5] Bonner J C and Blöte H 1982 *Phys. Rev.* B **25** 6959–80
[6] Kittel C 1968 *Introduction to Solid State Physics* 3rd edn (New York: Wiley)
[7] Silberglitt R and Torrance J B Jr 1970 *Phys. Rev.* B **2** 772–8
[8] Papanicolaou N and Psaltakis G C 1987 *Phys. Rev.* B **35** 342–51
[9] Regnault L P, Rossat-Mignod J, Renard J P, Verdaguer M and Vettier C 1989 *Physica* B **156–157** 247–53
[10] Torrance J B Jr and Tinkham M 1969 *Phys. Rev.* **187** 595–606
[11] Haldane F D M 1982 *J. Phys. C: Solid State Phys.* **15** L1309–13
[12] Haldane F D M 1983 *Phys. Lett.* **93A** 464–8; 1983 *Phys. Rev. Lett.* **50** 1153–6
[13] Krivoruchko V N 1988 *Sov. J. Low Temp. Phys.* **14** 464–7